



COVER PICTURE

The cover picture shows as grown garnet $Y_3Al_5O_{12}$ (YAG): Co, Si single crystals obtained by the Czochralski method with a diameter of 2 cm. From left till right:

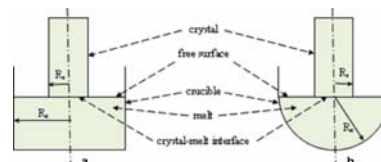
- YAG: 0.4 at.%Co,
 - YAG: 0.4 at.%Co, 0.2 at.%Si,
 - YAG: 0.8 at.%Co, 0.4 at.%Si.
- (see pages 823 – 833).

ORIGINAL PAPERS

Page **787–799** _____ F. Mokhtari, A. Bouabdallah, M. Zizi, S. Hanchi, and A. Alemany

Combined effects of crucible geometry and Marangoni convection on silicon Czochralski crystal growth

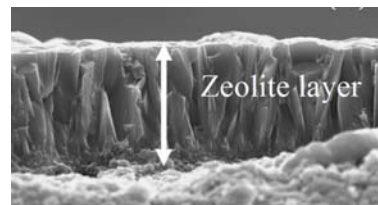
In order to understand the influence of crucible geometry combined with natural convection and Marangoni convection on melt flow pattern, temperature and pressure fields in silicon Czochralski crystal growth process, a set of numerical simulations was conducted. We carry out calculation enable us to determine temperature, pressure and velocity fields in function of Grashof and Marangoni numbers ...



Page **800–806** _____ B. Soydaş, P. Z. Çulfaz, H. Kalıpçılar, and A. Çulfaz

Crystallization of silicalite-1 from clear synthesis solutions: Effect of template concentration on crystallization rate and crystal size

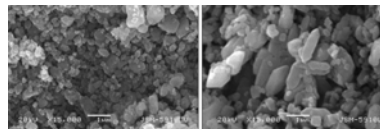
Synthesis of silicalite-1 powders and membranes from initially clear solutions with different tetrapropylammonium hydroxide or bromide concentrations was studied. While tetrapropylammonium bromide acts only as template, tetrapropylammonium hydroxide provides both the template and hydroxyl ions to the synthesis medium. The effects of template and hydroxyl ion concentration on the product yield, crystallization rate and crystal size were investigated ...



Page **807–817** _____ P. Sayan, S. Titiz Sargut, and B. Kiran

Calcium oxalate crystallization in the presence of amino acids, proteins and carboxylic acids

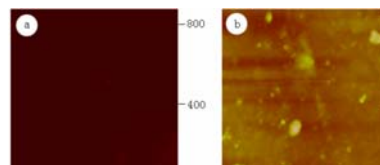
Reactive crystallization of calcium oxalate was investigated in the presence of amino acids, proteins and carboxylic acids at different pH and temperatures. Average particle size, filtration rates of calcium oxalate crystals obtained in the absence and presence of additives were ...



Page **818–822** _____ Fangzhi Huang, Yuhua Shen, Anjian Xie, Xiuzhen Zhang, Yan Cai, and Wenting Wu

Controlled deposition and transformation of amorphous calcium carbonate thin films

Controlled synthesis of amorphous calcium carbonate (ACC) films was realized by using the multiple templates, which are composed of a self-assembled film (SAF, insoluble Poly (ϵ -caprolactone) film) and a soluble modifier (poly allylamine), as modifiers. The formation of self-assembled film was analyzed by monitoring the morphologies ...



Page **823–833** _____ E. Talik, M. Szubka, D. Skrzypek, W. Zarek, J. Kusz, and T. Łukasiewicz

SQUID magnetometry, EPR and XPS characterization of $Y_3Al_5O_{12}$: Co, Si single crystals

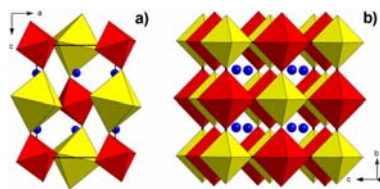
Single crystals of garnet $Y_3Al_5O_{12}$ (YAG): Co and Co, Si were grown by Czochralski method as materials for optoelectronic applications. Silicon doping is responsible for the change of the Co^{3+} ions into Co^{2+} in order to keep charge neutrality of the material and for a coloration of materials. Magnetization and Electron Paramagnetic Resonance measurements show that the most cobalt ions in the silicon co-doped crystals ...



Page **834–840** _____ E. Smrčok, M. Kucharik, M. Tovar, and I. Žižak

High temperature powder diffraction and solid state DFT study of β -cryolite (Na_3AlF_6)

Neutron and synchrotron powder diffraction data for β -cryolite were collected within 550–800(880) °C. Atomic coordinates of Al, F and Na atoms were obtained by both neutron Rietveld refinement and energy minimization in solid state at DFT level of theory. It was shown that although Rietveld refinements with fluorine atoms statically ...



Page **841–844** _____ Zhongchun Li, Aijun Gu, and Quanfa Zhou

Growth of spindle-shaped silver nanoparticles in SDS solutions

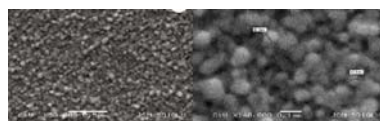
Spindle-shaped silver nanoparticles were successfully prepared in high yield by a simple wet chemical approach using citric acid (CA) as reductant in the presence of sodium dodecyl sulfate (SDS) at room temperature. Transmission electron microscopy (TEM), UV-vis absorption spectroscopy and X-ray diffraction ...



Page **845–850** _____ Z. K. Heiba and L. Arda

Structural properties of $Zn_{1-x}Mg_xO$ nanomaterials prepared by sol-gel method

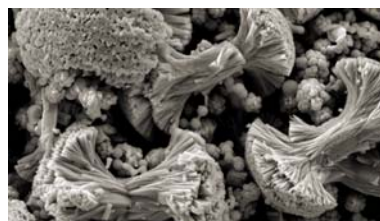
The mixed oxides $Zn_{1-x}Mg_xO$ (ZMO) were prepared as nano-polycrystalline powders and thin films by a simple sol-gel process and dip coating method. Thermogravimetric (TG) and differential thermal analysis (DTA) were used to study the thermal chemistry properties of dried gel. Structural and microstructural analysis was carried out ...



Page **851–856** _____ Yongbin Xu, Zhongming Ren, Guanghui Cao, Weili Ren, Kang Deng, and Yunbo Zhong

A template-free route for controlled synthesis of dumbbell-like Sb_2S_3 microcrystals

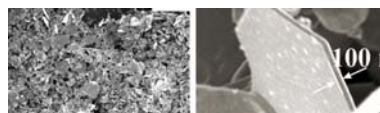
Large amounts of dumbbell-like Sb_2S_3 microcrystals were synthesized via a simple solvothermal treatment method. Various techniques such as x-ray diffraction (XRD), field-emission scanning electron microscope (FESEM), high-resolution transmission electron microscope (HRTEM), selected area electron diffraction (SAED), and photoluminescence spectrometry (PL) have been used to characterize the obtained products. The results showed that the products belong to the orthorhombic ...



Page **857–860** _____ Ting You, Sixiu Sun, Xinyu Song, and Shuling Xu

Simple extraction-solvothermal synthesis of single-crystalline silver microplates

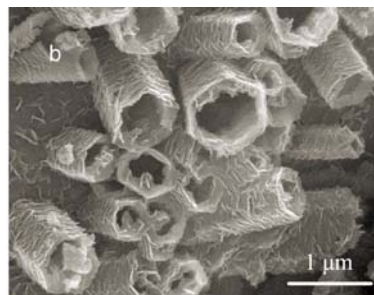
Single-crystalline silver microplates, with average edge length of about 1.5 μm and thickness of 100 nm, have been synthesized by a simple extraction-solvothermal method. Samples were characterized in detail by X-ray diffraction (XRD), field-emission scanning electron microscopy (FE-SEM), transmission electron microscopy (TEM) and High-resolution transmission electron microscopy (HRTEM) ...



Page **861–864** _____ Xiaoqun Wei, Haichao Li, Shuixia Chen, Chane Yuan, and Qingyu Yuan

One-step synthesis of ZnO/MgO core-sheath structures

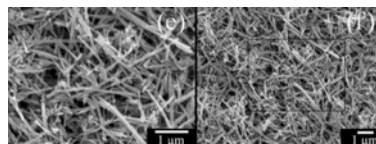
A kind of ZnO/MgO core-sheath structure has been prepared directly by the pyrolysis of a mixture of polyvinyl alcohol, magnesium acetate, and zinc chloride coating on glass fiber mats at 450 °C for 60 min. The growing process and effect of the anions on the morphology of ZnO/MgO structures have been preliminarily discussed. The results indicate that ZnCl₂ will transform to ...



Page **865–869** _____ Titipun Thongtem, Anukorn Phuruangrat, and Somchai Thongtem

Solvothermal production of CdS nanorods using polyvinylpyrrolidone as a template

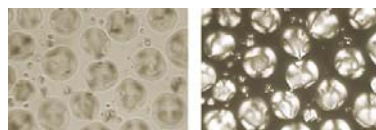
CdS nanorods were solvothermally produced using Cd(NO₃)₂ and S powder in ethylenediamine containing different amounts of polyvinylpyrrolidone (PVP). The phase with hexagonal structure was detected using X-ray diffraction (XRD) and selected area electron diffraction (SAED). Their SAED patterns were in accordance with those of the simulations ...



Page **870–878** _____ Y. G. Marinov, G. B. Hadjichristov, and A. G. Petrov

Single-layered microscale linear-gradient PDLC material for electro-optics

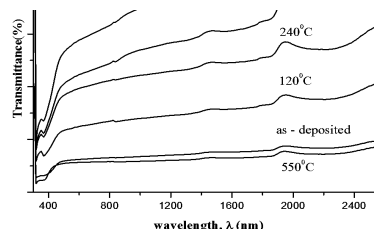
We report on single-layered optical material of linear-gradient microscale polymer-dispersed liquid crystal (PDLC). E7/NOA65 composite films formed by pulsed UV laser photopolymerization-induced phase separation exhibit two morphology types, namely a bipolar and a hybrid alignment of liquid crystal droplets. The specific structural properties of the ...



Page **879–882** _____ T. Ghosh, S. Bandopadhyay, K. K. Roy, A. K. Maiti, and K. Goswami

Optical studies on ZnO films prepared by sol-gel method

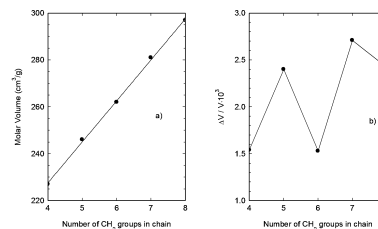
A standard sol-gel method was used to deposit ZnO thin films of suitable thickness on glass substrate. The optical characteristics of the visible to infrared range on thermal stress were critically observed. Morphological signature of the films was detected by X-ray diffraction (XRD) and the crystallite size determined by Scherrer ...



Page 883–888 _____ I. Zgura, R. Moldovan, T. Beica, and S. Frunza

Temperature dependence of the density of some liquid crystals in the alkyl cyanobiphenyl series

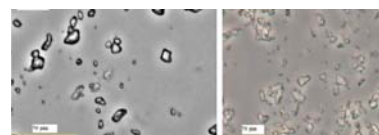
Experimental results for the temperature dependence of the density of propyl - cyanobiphenyl (3CB), butyl - cyanobiphenyl (4CB) and hexyl - cyanobiphenyl (6CB) are presented. The results are compared with previous results for temperature dependence of other members of the alkyl cyanobiphenyl series (nCB). The deviation of the density from linear temperature dependence is discussed in terms of the recently discovered corresponding rule for nematic liquid



Page 889–896 _____ S. R. Patel and Z. V. P Murthy

Ultrasound assisted crystallization for the recovery of lactose in an anti-solvent acetone

Continuous worldwide increase in high-scale production of dairy products leads to the constant generation of vast amounts of liquid by-product, whey. Disposal of liquid whey is costly due to its high biological oxygen demand (BOD) and water content. More than 90% of whey BOD is due to lactose. Recovery of lactose from whey solves both the problems of improving ...



Crystal Research and Technology is indexed in Cambridge Scientific Abstracts, CCR Database, Chemical Abstracts Service/SciFinder, ChemInform, Chemistry Citation Index™, Chemistry Server Reaction Center, Chimica Database, COMPENDEX, CSA Technology Research Database, Current Contents®/Physical, Chemical & Earth Sciences, FIZ Karlsruhe Databases, INSPEC, Journal Citation Reports/Science Edition, Materials Science Citation Index®, Reaction Citation Index™, Science Citation Index Expanded™, Science Citation Index®, SCOPUS, VINITI, Web of Science®